

Quantum computation with doped silicon cavities

M. Abanto,* L. Davidovich, Belita Koiller, and R. L. de Matos Filho

Instituto de Física, Universidade Federal do Rio de Janeiro, Caixa Postal 68528, Rio de Janeiro 21941-972, RJ, Brazil

(Received 4 November 2009; revised manuscript received 8 January 2010; published 18 February 2010)

We propose an architecture for quantum computing involving substitutional donors in photonic-crystal silicon cavities and the optical initialization, manipulation, and detection processes already demonstrated in ion traps and other atomic systems. Our scheme leads to easily achievable requirements on the positioning of the donors and considerably simplifies the implementation of the building blocks required for the operation of silicon-based quantum computing devices, including realization of one- and two-qubit gates, initialization, and readout of the qubits. Detailed consideration of the processes involved, using state-of-the-art values for the relevant parameters, indicates that this architecture leads to errors per gate compatible with fault-tolerant quantum computation and should be useful for quantum simulations and quantum optics applications.

DOI: [10.1103/PhysRevB.81.085325](https://doi.org/10.1103/PhysRevB.81.085325)

PACS number(s): 71.55.Cn, 03.67.Lx, 42.50.Pq

I. INTRODUCTION

The search for a working quantum computer (QC) has comprised areas ranging from optics to atomic and condensed-matter physics.¹ Finding physical systems that allow for accurate operations has been a formidable challenge, yet to be met. Indeed, the viability of quantum computers depends on finding physical systems that allow scalable fault-tolerant computation, which means that the errors remain bounded when the number of qubits increases. In order to have scalable quantum computation, the error per gate should be smaller than a certain threshold, which depends on the specific error-correction scheme. For independent and identically distributed errors, the best lower bound so far is 1.9×10^{-4} .² For other architectures, which require however a large resource overhead,³ this threshold is bounded below by 1.04×10^{-3} .⁴ Recent schemes keep lower bounds $\leq 10^{-3}$ within significantly reduced overhead requirements.⁵

Many physical systems have been proposed as candidates for qubits in a QC. The first experimental demonstration of a quantum gate involved an ion trap,⁶ and ion traps are currently the leader in terms of number of addressable and interacting qubits.⁷⁻⁹ Multiparticle quantum control is obtained by confining ions in an electromagnetic trap and manipulating them with laser pulses. The qubit states are taken as two hyperfine states of an ion (beryllium, for example). Experimental advances in solid-state proposals are still focused at the one- and two-qubit levels.^{10,11}

The perspective of benefiting from the available microelectronics technology brings continuous attention from the QC community to semiconductor quantum devices,¹²⁻¹⁴ particularly those based on silicon.¹⁵⁻²⁵ Successful experimental efforts in single donor control demonstrate the potential of isolated donors in Si for applications in electronic nanodevices.²⁶⁻³⁰ Most candidates for such devices rely on spin-1/2 fermions^{12,31} which for Si may be associated to the long-lived electron and nuclear spins of shallow substitutional donors.^{15,32} In fact, electronic spin decoherence times have been shown to be larger than 60 ms in ²⁸Si (isotopically purified) at temperatures of 7 K.^{33,34} Implementation of quantum computation with these systems is hindered by several problems. The most obvious difficulty with spin qubits¹⁰

regards the manipulation and measurement of single-spin states. Two-qubit operations relying on exchange gates,¹² restricted to nearest-neighbor interactions, have limited scalability potential.³⁵ Moreover the particular electronic band structure of bulk Si leads to fast oscillations in the electronic exchange coupling when the interacting donor-pair relative position is changed on a lattice-parameter scale.³⁶ Thus, proposals based on this mechanism require nanofabrication techniques far beyond current capabilities.

In this work we propose combining the Si substitutional-donor QC architecture, where qubits are encoded in group-V donor-electron-spin states, with the optical initialization and manipulation processes already demonstrated in ion traps and other atomic schemes. The qubits are taken as the donor ground-state Zeeman-split levels, labeled by $|\uparrow\rangle$ and $|\downarrow\rangle$, which result from the interaction of the electron spin with a uniform magnetic field (B) strong enough to overcome the hyperfine coupling. Donors are placed in a single-mode photonic-crystal Si cavity³⁷ and are optically addressed through Raman transitions induced by the cavity mode and only three applied laser beams, spread out over the whole ensemble. The system is kept at a temperature near 7 K. A fourth laser beam is used for the readout. Essential elements of the proposed architecture are schematically illustrated in Fig. 1, where we represent an array of donors positioned at the antinodes of the cavity mode. One- and two-qubit logical gates, as well as system initialization and readout, are implemented through the external laser beams, which address all qubits simultaneously. The coupling between a donor electron and the light fields may be interrupted by an external electric field, due to the Stark shift of the donor levels. This effect is explored for selecting the target qubits for one- or two-qubit operations. Two-qubit operations are mediated by the vacuum field of the photonic-crystal cavity.¹³

The coherent control and manipulation of donors in Si by optical means has been recently demonstrated,³⁸ thus opening the way for extending to this system the techniques applied to trapped ions. This reinforces the viability and interest of our proposal.

This paper is organized as follows: in Sec. II we briefly review the electronic properties of shallow donors in Si, defining the relevant orbital levels for the scheme proposed here. The spin qubit states are presented in Sec. III. Qubit

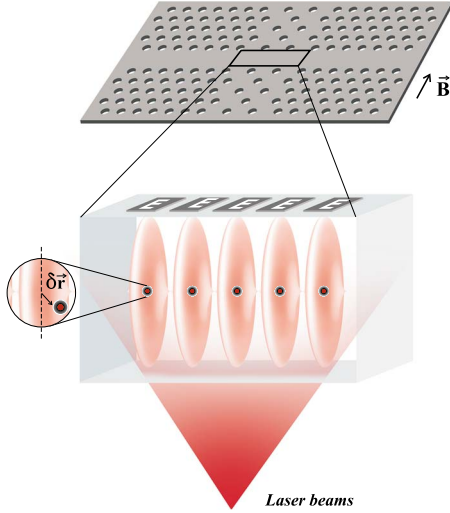


FIG. 1. (Color online) Schematic representation of the QC architecture proposed here. Donor impurities are placed in the neighborhood of intensity maxima of a photonic-crystal cavity mode, not necessarily every maximum. The donors are under the action of a uniform magnetic field \mathbf{B} and electric fields \mathbf{E} , produced by the electrodes E . The magnetic field is strong enough to decouple nuclear and electronic spins in the donor ground state, and Zeeman splits two electronic spin states, $|\uparrow\rangle$ and $|\downarrow\rangle$, which constitute the qubit. Turning on the electric fields allows us to switch off individual qubit Raman transitions induced by the two laser beams, spread out over the ensemble of qubits, and also the coupling among different qubits through the vacuum cavity field. The inset displays the misplacement $\delta\mathbf{r}$ of an impurity from a maximum of the cavity mode.

selectivity, optically driven processes leading to the required logical gate operations, initialization and readout are discussed in Sec. IV. Errors estimates from different processes, including errors due to displacements of the donors with respect to ideal positioning, are discussed in Sec. V. Summary and final remarks are presented in Sec. VI.

II. SHALLOW SUBSTITUTIONAL DONORS IN SI

The study of group-V donor impurities in silicon is a quite mature field.^{39,40} When a group-V element, such as P, As, or Sb, substitutes the group-IV Si atom in bulk Si, an additional electron is incorporated in the system, which remains bound to the core potential via a screened Coulomb interaction. This system constitutes a solid-state analog of the hydrogen atom⁴⁰ and the theory for the binding energies and symmetries of donor electronic states in Si is conveniently formulated within the so-called effective-mass approximation (EMA). The simplest EMA (single valley) formulation consists in considering the energy eigenfunctions as products of bulk Bloch functions at the conduction-band minimum, $\psi_{\mathbf{k}_\mu}(\mathbf{r}) = u_{\mathbf{k}_\mu}(\mathbf{r}) e^{i\mathbf{k}_\mu \cdot \mathbf{r}}$, by envelope functions $F_\mu(\mathbf{r})$, which are slowly varying at the lattice-parameter scale.³⁹ The bottom of the conduction band of Si is sixfold degenerate, with minima at reciprocal-space points \mathbf{k}_μ located along six equivalent directions in the Si lattice conventional cubic cell directions, $\mu = \pm x, \pm y,$ and $\pm z$. The conduction-band dispersion

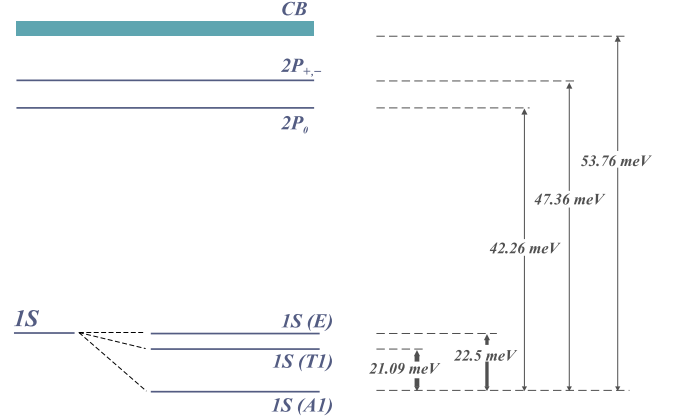


FIG. 2. (Color online) Experimental values, from Ref. 40, for orbital energy levels of As in Si. Only the levels relevant for the present study are shown. Here CB stands for conduction band.

around \mathbf{k}_μ is anisotropic and may be described in terms of longitudinal and transverse effective masses with respect to the μ axes, m_ℓ and m_t , so that the envelopes satisfy a hydrogeniclike Schrödinger equation. For example, for $\mu = z$,

$$-\left[\frac{\hbar^2}{2m_t} \left(\frac{\partial^2}{\partial x^2} + \frac{\partial^2}{\partial y^2} \right) + \frac{\hbar^2}{2m_\ell} \frac{\partial^2}{\partial z^2} + \frac{e^2}{\epsilon r} \right] F_z(\mathbf{r}) = EF_z(\mathbf{r}), \quad (1)$$

where $m_\ell = 0.98m_0$ and $m_t = 0.19m_0$, where m_0 is the free-electron mass and $\epsilon = 11.4$ is the Si dielectric constant. Note that Eq. (1) has axial symmetry rather than spherical and the effective Hamiltonian commutes only with the z component of the angular momentum. States with magnetic quantum numbers $\pm m$ are degenerate by time-reversal symmetry. Thus the $2p$ -like levels, which are triply degenerate for spherical symmetry (when $m_\ell = m_t$) split here into a singlet $2P_0$ with $m = 0$ and a doublet $2P_\pm$ with $m = \pm 1$. The EMA effective Hamiltonian has inversion symmetry, thus electric dipole transitions originating from the $1S$ ground state are allowed only into odd-parity excited states, in particular, $2P_\pm$ and $2P_0$.

Note that there are six equations equivalent to Eq. (1), thus each hydrogeniclike donor state, e.g., $1S$ and $2P_0$, is sixfold degenerate. The degeneracy of the $1S$ states is partially lifted due to the local crystal potential of tetrahedral symmetry, leading to a singlet $1S(A1)$, a doublet $1S(E)$, and a triplet $1S(T_2)$, where the notation specifies the state symmetry according to the tetrahedral symmetry group. Particularly the nondegenerate level $1S(A1)$ is the absolute ground state.³⁹ Experimental values for As donors give the $A1$ state 21.1 meV below the T_2 state of the $1S$ manifold and 53.7 meV below the bottom of the Si conduction band. It is also important to point out that the singlet $1S(A1)$ state is 47.36 meV below the $2P_\pm$ states. See Fig. 2 for an schematic representation of the energy levels for the case of As. Central cell corrections are negligible for the excited states.⁴⁰

In general a donor-electron wave function can be written as

$$\Psi(\mathbf{r}) = \sum_{\mu=1}^6 \alpha_{\mu} \psi_{\mathbf{k}_{\mu}}(\mathbf{r}) F_{\mu}(\mathbf{r}), \quad (2)$$

where the valley populations $\{\alpha_{\mu}\}$ satisfy the condition $\sum_{\mu=1}^6 |\alpha_{\mu}|^2 = 1$ and specify the symmetry of the state according to the tetrahedral impurity environment. For the $1S(A1)$ state, $\alpha_{\mu} = 1/\sqrt{6}$ while the $2P_{\pm}$ states coefficients are consistent with the $2T_1 \oplus 2T_2$ symmetry.³⁹ For example, $\alpha_x = -\alpha_{-x} = 1/\sqrt{2}$ (and zero for the other valley components) for symmetry T_2 and $\alpha_x = \alpha_{-x} = 1/\sqrt{2}$ (and zero for the other valley components) for symmetry T_1 .

For the dipole transition matrix elements calculations we assume spherically symmetric envelopes, which is the simplest approximation and should give adequate order-of-magnitude estimates for the relevant processes considered below. Thus we take $F_{\mu}^{1S} = \frac{1}{(\pi a_B^3)^{1/2}} e^{-r/a_B}$ and $F_z^{2P_{\pm}} = \frac{\sqrt{6} a_B^{3/2}}{12} \frac{r}{a_B} e^{-r/2a_B} Y_1^{\pm 1}$, where $Y_1^{\pm 1}$ are spherical harmonics. The effective Bohr radius is taken as $a_B = (a^2 b)^{1/3} = 20.7 \text{ \AA}$, where a and b are anisotropic Bohr radii obtained variationally.³⁹

III. DONOR ELECTRON SPIN STATES AS QUBITS

Qubit states are defined within the $1S(A1)$ ground state (see Fig. 2) under a magnetic field B satisfying $g_e \mu_B B \gg A$, where A is the hyperfine coupling constant, μ_B is the Bohr magneton, and $g_e (\approx 2)$ is the electron Landé factor in Si. In the absence of B , $1S(A1)$ accommodates a hyperfine manifold where the electron and nuclear spins are coupled via A . For a large enough magnetic field, meeting the above condition, electron and nuclear spins decouple and the ground state splits into two levels of well-defined electronic spins: $|\downarrow\rangle$ and $|\uparrow\rangle$, which may define the qubit logical states $|0\rangle$ and $|1\rangle$. Access and control over qubit superposition states, essential for QC, requires here a spin-flip interaction: We propose the spin-orbit (SO) interaction in the $2P_{+,-}$ manifold to mediate the coupling of the opposite-spin qubit states. This restricts the possible choices for shallow donor species, in particular, excluding P, the lighter among the group-V shallow donors in Si, with negligible SO coupling.⁴¹ Among the heavier group-V shallow donors, we propose here As since this species has a single stable isotope of nuclear spin $3/2$ while natural Sb has two stable isotopes of nuclear spins $3/2$ and $7/2$, thus with different hyperfine manifolds. Of course this difficulty may be overcome by applying a strong enough magnetic field but As seems to be a simpler choice. The SO interaction is estimated and further discussed in Sec. IV B. In what follows, we assume As donors for the quantitative data and estimates.

For As in Si, $A = 400 \text{ MHz}$, so a magnetic field $B = 0.3 \text{ T}$ will decouple nuclear and electron-spin states, generating electron-spin states $|\downarrow\rangle$ and $|\uparrow\rangle$ which define the qubits, with a 10 GHz splitting. Note that the qubit states are reasonably well separated from each other and both are about 5 THz (21 meV) lower in energy from the next excited state $1S(T1)$, as indicated in Fig. 2.

IV. LOGICAL GATES IN SILICON CAVITIES

A. Qubit selectivity

According to Barenco *et al.*,⁴² a system with gates that perform all one-qubit quantum operations and a single two-

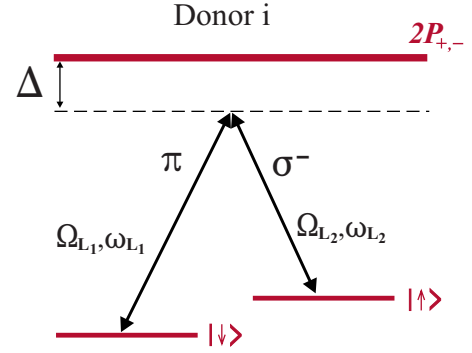


FIG. 3. (Color online) Representation of the logical gates for one-qubit operations. The arrows indicate Raman coupling of the qubit states $|\downarrow\rangle$ and $|\uparrow\rangle$ mediated by a linearly polarized laser beam and a circularly right-polarized beam. Spin flip is mediated by spin-orbit coupling in the $2P_{+,-}$ manifold.

qubit operation (e.g., XOR or C-NOT) is universal for quantum computing so that all unitary operations on any number of qubits can be performed as compositions of these elementary gates. Thus in a working QC only one-qubit operations or two-qubit operations need to be performed in the course of a running algorithm. Implementing the operations required in this protocol involves the capacity to individually select any qubit or pair of qubits in the device. In principle each E gate produces an electric field in the donor below it which Stark shifts the levels in the spectrum. In performing a given operation, the involved donors are previously selected by switching off the Stark-shift electric fields acting on them. Operations on spin qubits may require spin-flip processes, which are mediated here by the SO coupling in the $2P_{+,-}$ manifold, as discussed in Sec. IV B.

B. One-qubit operations

One-qubit operations are implemented through Raman coupling of the states $|\downarrow\rangle$ and $|\uparrow\rangle$ of donors previously selected by switching off the Stark-shift electric fields acting on them. In this excitation scheme, the donors interact with two laser fields of Rabi frequencies Ω_{L_1} and Ω_{L_2} , and frequencies ω_{L_1} and ω_{L_2} , respectively, detuned from the transitions between the qubit states $|\downarrow\rangle$ and $|\uparrow\rangle$ and the states $|2P_{+,-}\rangle$ by Δ , as shown in Fig. 3 (the fine-structure splitting of the levels $2P_{+,-}$ is not shown). The field with frequency ω_{L_1} is linearly polarized along the direction of the magnetic field, which also coincides with the direction of polarization of the cavity mode. The field with frequency ω_{L_2} is circularly right polarized. If $\Delta \gg \Omega_{L_1}, \Omega_{L_2}, \Gamma_p$, with Γ_p being the decay rate of the levels $2P_{+,-}$, the levels $2P_{+,-}$ are only virtually populated, giving rise to an effective coupling between levels $|\downarrow\rangle$ and $|\uparrow\rangle$, described, in the interaction picture, if $\Omega_{L_1} = \Omega_{L_2}$, by the Hamiltonian

$$\hat{H}_{\text{eff}} = \hbar \Omega_{\text{eff}} |\downarrow\rangle \langle \uparrow| + \text{H.c.}, \quad (3)$$

where $\Omega_{\text{eff}} = |\Omega_{L_1}|^2 / \Delta$.

During the Raman coupling of the qubit states there is a small probability, on the order of $\Omega_{\text{eff}} / \Delta$, of populating the

intermediate level $2P_{+,-}$. This will lead to decoherence of the one-qubit operations with the rate $\Omega_{\text{eff}}(\Gamma_p/\Delta)$ due to the spontaneous decay of the level $2P_{+,-}$. Since the time required for one-qubit operations is on the order of $1/\Omega_{\text{eff}}$, the error probability per gate will be $\epsilon_1 \approx \Gamma_p/\Delta$.

We propose a SO mediated coupling for the opposite-spin qubit states. In order to avoid destructive interference effects that would make Ω_{eff} vanishingly small, the intensity ζ of the SO coupling among the states within the $2P_{+,-}$ manifold must be comparable or larger than the detuning Δ of the laser fields. Strong SO splittings have been measured for states of the fundamental manifold in the group VI donors Si:Se and Si:Te, and of their corresponding ionized states.^{43–45} For Si:Se, the measured SO coupling is 3.2 cm^{-1} (96 GHz); so we assume in our calculations for As, the element corresponding to the Se row in the periodic table, a coupling of the same order of magnitude, $\zeta \sim 100 \text{ GHz}$.

The SO coupling also mediates an efficient mechanism for selectively turning on and off the interaction between the qubits and the light fields through an applied electric field produced by the electrode above each donor. The electric field has two effects: it increases the detuning between the Raman laser fields and the atomic transition so that it becomes much higher than the SO splitting, and it mixes $2P$ and $2S$ states. The increase in the detuning causes a destructive interference between the $2P$ states, which leads to the vanishing of the Raman transition. The mixing of $2P$ and $2S$ states also reduces the Raman coupling, since the $2S$ state does not couple with the ground state. Perturbation theory indicates that the combined effect reduces the transition probability by a factor equal to the third power of the ratio between the SO coupling and the electric dipole energy, which leads to an error on the order of 10^{-4} for an applied field equal to 20 kV/cm. This field is below the ionization threshold for P in Si (Ref. 46) and for As the threshold should be even higher since the binding energies are larger. Only the donors that are subjected to smaller electric fields will be affected by the Raman coupling. This scheme has the advantage that only quiescent atoms are subject to large electric fields so that the essential properties of the active atoms remain unchanged.

As detailed in the following section, the frequency of the cavity field is close to ω_{L_2} , so one must make sure that this field does not interfere with the one-qubit operations. Indeed, the assumption that the linearly polarized field is along the direction of the applied magnetic field and that the cavity mode is also linearly polarized along the same direction, implies, due to selection rules, that the cavity mode does not affect the one-qubit operations described above.

C. Two-qubit operations

Two-qubit operations involve the interaction of a previously Stark-shift-selected pair of qubits with an additional laser beam and with the cavity mode. The frequencies and polarizations of the laser and cavity fields are chosen in such a way that they nearly satisfy the conditions for Raman coupling of the qubit states $|\downarrow\rangle$ and $|\uparrow\rangle$ for each donor¹³ (see Fig. 4). The wavelength for the transition $1S(A_1) \rightarrow 2P_{+,-}$ is

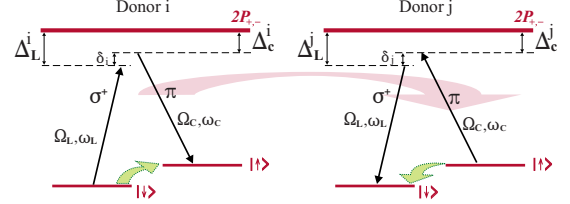


FIG. 4. (Color online) Diagram illustrating the logical gates for two-qubit operations. A linearly polarized cavity field along the direction of the magnetic field and a circularly left-polarized laser beam are represented by straight arrows. The long curved arrow indicates the effective two-qubit interaction mediated by the vacuum of the cavity mode. Short curved arrows give the net effect of the complete circle: $|\downarrow_i \uparrow_j\rangle \rightarrow |\uparrow_i \downarrow_j\rangle$. i.e., qubit states of donors i and j undergo a SWAP operation.

$26.39 \mu\text{m}$ in vacuum; in Si (dielectric constant $\epsilon=11.4$), the corresponding value is $\lambda=7.82 \mu\text{m}$. The wavelengths of the cavity mode and the laser beams should be around this value.

Under the conditions established for a Raman transition and in the dispersive regime, i.e., $\Delta_L^i \gg \Omega_L$, Γ_p and $\Delta_C^i \gg \Omega_C$, Γ_p , Γ_C , where Ω_C quantifies the coupling with the cavity mode, with width Γ_C , the states $2P_{+,-}$ are only virtually occupied, giving rise to an effective coupling between the cavity mode and the qubit states which, in an adequate interaction picture, is described by the Hamiltonian,

$$\hat{H}_{\text{eff}} = \sum_i [\hbar \Omega_{\text{eff}}^i \hat{a} \hat{\sigma}_-^i e^{-i\delta^i t} + \text{H.c.}], \quad (4)$$

where \hat{a} is the annihilation operator for the cavity field, $\hat{\sigma}_-^i = |\downarrow\rangle_i \langle \uparrow|$ is the spin-flip operator for donor i , $\delta^i = \Delta_L^i - \Delta_C^i$, and the sum extends over all the donors selected by the electric static fields. The couplings Ω_{eff}^i are defined as

$$\Omega_{\text{eff}}^i = \frac{1}{2} \Omega_L \Omega_C^* \left(\frac{1}{\Delta_L^i} + \frac{1}{\Delta_C^i} \right). \quad (5)$$

If $\delta^i \gg \Omega_{\text{eff}}^i$, Γ_C , the cavity field will be only virtually excited and can be eliminated from the dynamics, leading to an effective two-qubit interaction mediated by the vacuum of the cavity mode,

$$\hat{H}_{ij} = \sum_{i \neq j} [\hbar \Omega_{ij} \hat{\sigma}_+^i \hat{\sigma}_-^j e^{i\delta^j t} + \text{H.c.}], \quad (6)$$

where $\delta^j = \delta^i - \delta^j$. From Eq. (6), one can see that each pair of qubits i and j that satisfies $\delta^i = \delta^j$ will resonantly interact through the Hamiltonian

$$\hat{H}_{ij} = \hbar \Omega_{ij} \hat{\sigma}_+^i \hat{\sigma}_-^j + \text{H.c.} \quad (7)$$

with the effective coupling constant $\Omega_{ij} = [\Omega_{\text{eff}}^i (\Omega_{\text{eff}}^j)^*] / \delta^j$. The qubit pairs for which $\delta^j \gg \Omega_{ij}$ will interact off-resonantly and will not couple to each other. The error probability per gate for two-qubit operations can be found in a similar way as for one-qubit operations and will be given by $\epsilon_2 \approx \Gamma_C / \delta^j$.

Hamiltonian (7) implements the $\sqrt{\text{SWAP}}$ operation $|\uparrow\downarrow\rangle \rightarrow (|\uparrow\downarrow\rangle + |\downarrow\uparrow\rangle) / \sqrt{2}$, which, combined with single-qubit rotations, can be used to implement a C-NOT gate.¹² $\sqrt{\text{SWAP}}$

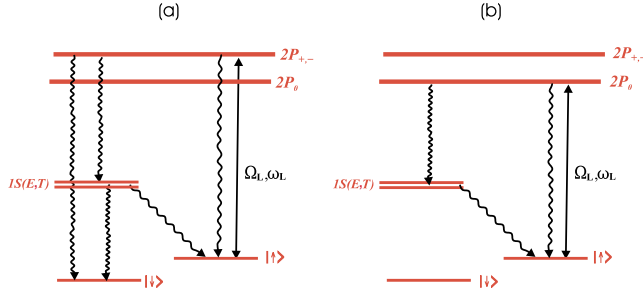


FIG. 5. (Color online) (a) Initialization: population of qubit state $|\uparrow\rangle$ is transferred to the qubit state $|\downarrow\rangle$ via optical pumping by resonantly exciting transition $|\uparrow\rangle \leftrightarrow 2P_{+,-}$ with laser light; (b) readout of the qubit state is made by monitoring the fluorescence light of the cyclic transition $|\uparrow\rangle \leftrightarrow 2P_0$.

operations can be implemented in parallel, by having different pairs, with $\delta^i = \delta^j$ and $\delta^k = \delta^l$, but $|\delta^i - \delta^k| \gg |\Omega_{ij}|$.

D. Initialization and readout

The qubits are initialized by driving resonantly the transition $|\uparrow\rangle \leftrightarrow 2P_{+,-}$ with a laser beam. Under the action of the magnetic field B and at temperatures on the order of 7 K only the state $1S(A1)$ will be populated. Since the level $2P_{+,-}$ is unstable, it will eventually decay to one of the qubit levels, through the levels $1S(E, T)$, leading to optical pumping of the level $|\downarrow\rangle$ [see Fig. 5(a)].

Qubit readout takes advantage of the fact that the states of the $2P_0$ manifold do not show SO coupling. If laser light excites resonantly the transition $|\uparrow\rangle \leftrightarrow 2P_0$, only the states of that manifold with the same electronic spin as the state $|\uparrow\rangle$ are excited. Due to selection rules, the radiative- or phonon-assisted decay of these states to states with different electronic spin is forbidden. The decay out of the $2P_0$ level is both radiative and phonon assisted, whereas the decay out of level $1S(E)$ is phonon assisted. For this reason, all the excitation will decay back to the state $|\uparrow\rangle$. Therefore the transition $|\uparrow\rangle \leftrightarrow 2P_0$ is cyclic and the electron shelving technique can be used to measure the occupation of the qubit states:⁴⁷ if, during the laser excitation of the transition $|\uparrow\rangle \leftrightarrow 2P_0$ fluorescence light is observed, the qubit was in state $|\uparrow\rangle$, otherwise the state $|\downarrow\rangle$ was occupied [see Fig. 5(b)]. Since the decay $1S(E) \rightarrow |\uparrow\rangle$ is assisted by acoustic phonons, the fluorescence light differs in frequency from the laser exciting the transition $|\uparrow\rangle \leftrightarrow 2P_0$, which implies that it is possible to distinguish the fluorescence signal from scattered laser radiation.

V. FEASIBILITY AND ERROR ESTIMATES

The feasibility of the proposed scheme is based on the following estimates for the frequencies, couplings, and times involved in the one-qubit, two-qubit, and readout operations. The measured absorption linewidth of the $1S(A1) \rightarrow 2P_{+,-}$ transition for Si:P is approximately 1GHz,⁴⁸ giving an upper bound for the decay rate Γ_p . This rate could be strongly decreased (more than one order of magnitude) since phonon-mediated decay can be suppressed by applying stress, as

demonstrated in Ref. 49, and spontaneous radiative transitions from these levels are also strongly suppressed due to the photonic band gap since they are far detuned from the cavity mode of the photonic crystal.⁵⁰ The Raman-coupling conditions are satisfied, for example, for $\Omega_{L_1}/2\pi = \Omega_{L_2}/2\pi = 2$ GHz and $\Delta = 200$ GHz. This would lead to an effective Rabi frequency $\Omega_{\text{eff}}/2\pi = 20$ MHz and an error probability per gate $\epsilon_1 \approx 10^{-4}$. For these parameters, which correspond to laser powers on the order of 10 mW, the typical time for a one-qubit operation would be on the order of 50 ns, much shorter than a spin decoherence time of 60 ms. Under the same conditions, we have calculated that the error probability per gate induced by eventual impurity ionization, due to two-photon absorption, is negligibly small ($\epsilon \approx 6 \times 10^{-7}$).

For the two-qubit operations, one may choose $\Omega_L^i/2\pi \sim 5$ GHz, $\Delta_L^i = 100$ GHz, $\Delta_C^i = 99$ GHz, and $\Omega_C^i/2\pi \sim 30$ MHz, which is compatible with oscillator strengths reported in the literature⁵¹ and a cavity modal volume of $100\lambda^3$. This modal volume would accommodate up to 400 qubits in a two-dimensional array. Smaller values of Ω_C^i could be compensated by larger intensities of the laser fields. This yields an effective two-qubit coupling $\Omega_{ij}/2\pi \sim 2.25$ KHz, which allows one to perform more than 10^3 $\sqrt{\text{SWAP}}$ operations within a qubit decoherence time of 60 ms. Since for two-qubit operations the error per gate is $\epsilon_2 \approx \Gamma_C/\delta_i$, an error per gate on the order of 1×10^{-3} would imply a cavity decay rate $\Gamma_C \approx 1$ MHz. This requires a cavity quality factor $Q \approx 10^7$. Quality factors of 10^6 have already been reported for silicon-based photonic-crystal nanocavities;³⁷ Q 's as high as 2×10^7 seem to be within reach.³⁷ Larger wavelengths in the micrometer region, as used in our proposal, should lead to yet higher values of Q . Combined with larger values of the spin decoherence time, consistent with the experimental results,^{33,52} this would allow one to increase δ , further reducing the error per gate.

Readout is very efficient and fast. Assuming an overall quantum efficiency of $\approx 10^{-4}$ for the photodetection system, we estimate that the scattering on the order of 2×10^5 photons by the transition $2P_0 \rightarrow 1S(E)$ [total decay rate of the order of 1 GHz (Ref. 53)] should yield a reading efficiency close to 100%. Parallel readout can be implemented for donors separated by ten cavity wavelengths or more.

Finally, we address a crucial fabrication issue: given that the best currently achievable deposition control for impurities in Si is ~ 10 Å,⁵⁴ the impact of small donor misplacements on the proposed device operation must be analyzed. A deviation $\delta\vec{r}$ in the position of a donor from a maximum of the cavity field (see Fig. 1) introduces a variation $\Delta\Omega_C \approx 2\pi^2(|\delta\vec{r}|/\lambda)^2\Omega_C$ on the cavity vacuum Rabi frequency Ω_C at the position of the donor. Here $\lambda = 7.8$ μm is the cavity wavelength. This implies that $|\delta\vec{r}| = 100$ Å leads to $\Delta\Omega_C \approx 3 \times 10^{-5}\Omega_C$. The time for a typical two-qubit gate such as $\sqrt{\text{SWAP}}$ is $t \sim 1/\Omega_{ij}$, leading to an error probability in this operation of $p \approx (\Delta\Omega_C/\Omega_C)^2 \approx 1 \times 10^{-9}$, which means that our operation scheme is quite insensitive to relatively large (several lattice parameters) donor misplacement within the simple donor linear array architecture. This is in contrast with Kane's original exchange-based proposal, which leads to much more stringent conditions on impurity positioning, and requires elaborate two-dimensional architectures to compensate for donor misplacement.⁵⁵

VI. FINAL REMARKS

In summary, our estimations show that the present proposal is compatible with errors per gate within bounds for fault-tolerant qubit operations.⁵ Further considering that: (i) precise quantum control of atoms and ions in optical cavities has already been demonstrated in several laboratories and optical manipulation of donors in Si are in many respects analogous to these systems (e.g., Ref. 38) and (ii) Si is the leading material in terms of processing and device fabrication, with sophisticated techniques for impurity implantation and high- Q microcavity construction, we may conclude that the system proposed here is a viable candidate for applica-

tions requiring a limited number of qubits, as, for example, the computation of molecular energies in quantum chemistry.⁵⁶

ACKNOWLEDGMENTS

The authors acknowledge financial support from the Brazilian agencies CNPq, CAPES, PRONEX, FUJB, and FAPERJ. This work was performed as part of the Brazilian Millennium Institutes for Quantum Information and Nanotechnology, and the National Institute of Science and Technology (INCT) for Quantum Information.

*Present address: CCBN, Universidade Federal do Acre, Cx. Postal 500, Rio Branco, AC 69915-900, Brazil.

- ¹M. Nielsen and I. Chuang, *Quantum Computation and Quantum Information* (Cambridge University Press, Cambridge, UK, 2000).
- ²P. Aliferis and A. W. Cross, *Phys. Rev. Lett.* **98**, 220502 (2007).
- ³E. Knill, *Nature (London)* **434**, 39 (2005).
- ⁴P. Aliferis, D. Gottesman, and J. Preskill, *Quantum Inf. Comput.* **8**, 181 (2008).
- ⁵P. Aliferis and J. Preskill, *Phys. Rev. A* **79**, 012332 (2009).
- ⁶C. Monroe, D. M. Meekhof, B. E. King, W. M. Itano, and D. J. Wineland, *Phys. Rev. Lett.* **75**, 4714 (1995).
- ⁷D. Leibfried, E. Knill, S. Seidelin, J. Britton, R. B. Blakestad, J. Chiaverini, D. B. Hume, W. M. Itano, J. D. Jost, C. Langer, R. Ozeri, R. Reichle, and D. J. Wineland, *Nature (London)* **438**, 639 (2005).
- ⁸H. Häffner, W. Hänsel, C. F. Roos, J. Benhelm, D. Chek-al-kar, M. Chwalla, T. Körber, U. D. Rapol, M. Riebe, P. O. Schmidt, C. Becher, O. Gühne, W. Dür, and R. Blatt, *Nature (London)* **438**, 643 (2005).
- ⁹D. Hanneke, J. P. Home, J. D. Jost, J. M. Amini, D. Leibfried, and D. J. Wineland, *Nat. Phys.* **6**, 13 (2010).
- ¹⁰B. E. Kane, *MRS Bull.* **30**, 105 (2005).
- ¹¹F. Brito, D. P. DiVincenzo, R. H. Koch, and M. Steffen, *New J. Phys.* **10**, 033027 (2008).
- ¹²D. Loss and D. P. DiVincenzo, *Phys. Rev. A* **57**, 120 (1998).
- ¹³A. Imamoglu, D. D. Awschalom, G. Burkard, D. P. DiVincenzo, D. Loss, M. Sherwin, and A. Small, *Phys. Rev. Lett.* **83**, 4204 (1999).
- ¹⁴M. S. Sherwin, A. Imamoglu, and T. Montroy, *Phys. Rev. A* **60**, 3508 (1999).
- ¹⁵B. E. Kane, *Nature (London)* **393**, 133 (1998).
- ¹⁶B. E. Kane, *Fortschr. Phys.* **48**, 1023 (2000).
- ¹⁷R. Vrijen, E. Yablonovitch, K. Wang, H. W. Jiang, A. Balandin, V. Roychowdhury, T. Mor, and D. DiVincenzo, *Phys. Rev. A* **62**, 012306 (2000).
- ¹⁸T. D. Ladd, J. R. Goldman, F. Yamaguchi, Y. Yamamoto, E. Abe, and K. M. Itoh, *Phys. Rev. Lett.* **89**, 017901 (2002).
- ¹⁹D. Mozyrsky, V. Privman, and M. L. Glasser, *Phys. Rev. Lett.* **86**, 5112 (2001).
- ²⁰J. Levy, *Phys. Rev. A* **64**, 052306 (2001).
- ²¹M. Friesen, P. Rugheimer, D. E. Savage, M. G. Lagally, D. W. van der Weide, R. Joynt, and M. A. Eriksson, *Phys. Rev. B* **67**, 121301(R) (2003).
- ²²A. J. Skinner, M. E. Davenport, and B. E. Kane, *Phys. Rev. Lett.* **90**, 087901 (2003).
- ²³A. M. Stoneham, A. J. Fisher, and P. T. Greenland, *J. Phys.: Condens. Matter* **15**, L447 (2003).
- ²⁴L. C. L. Hollenberg, A. S. Dzurak, C. Wellard, A. R. Hamilton, D. J. Reilly, G. J. Milburn, and R. G. Clark, *Phys. Rev. B* **69**, 113301 (2004).
- ²⁵R. de Sousa, J. D. Delgado, and S. Das Sarma, *Phys. Rev. A* **70**, 052304 (2004).
- ²⁶C. B. Simmons, M. Thalakulam, N. Shaji, L. J. Klein, H. Qin, H. Luo, R. H. Blick, D. E. Savage, M. G. Lagally, S. N. Copper-smith, and M. A. Eriksson, *Appl. Phys. Lett.* **91**, 213103 (2007).
- ²⁷G. P. Lansbergen R. Rahman, C. J. Wellard, I. Woo, J. Caro, N. Collaert, S. Biesemans, G. Klimeck, L. C. L. Hollenberg, and S. Rogge, *Nat. Phys.* **4**, 656 (2008).
- ²⁸C. C. Lo, A. Persaud, S. Dhuey, D. Olynick, F. Borondics, M. C. Martin, H. A. Bechtel, J. Bokor, and T. Schenkel, *Semicond. Sci. Technol.* **24**, 105022 (2009).
- ²⁹W. H. Lim, F. A. Zwanenburg, H. Huebl, M. Möttönen, K. W. Chan, A. Morello, and A. S. Dzurak, *Appl. Phys. Lett.* **95**, 242102 (2009).
- ³⁰K. Y. Tan, K. W. Chan, M. Möttönen, A. Morello, C. Yang, J. van Donkelaar, A. Alves, J.-M. Pirkkalainen, D. N. Jamieson, R. G. Clark and A. S. Dzurak, *Nano Lett.*, **10**, 1115 (2010).
- ³¹J. R. Petta, A. C. Johnson, J. M. Taylor, E. A. Laird, A. Yacoby, M. D. Lukin, C. M. Marcus, M. P. Hanson, and A. C. Gossard, *Science* **309**, 2180 (2005).
- ³²J. J. L. Morton, A. M. Tyryshkin, R. M. Brown, S. Shankar, B. W. Lovett, A. Ardavan, T. Schenkel, E. E. Haller, J. W. Ager, and S. A. Lyon, *Nature (London)* **455**, 1085 (2008).
- ³³A. M. Tyryshkin, S. A. Lyon, A. V. Astashkin, and A. M. Raitsimring, *Phys. Rev. B* **68**, 193207 (2003).
- ³⁴A. M. Tyryshkin, J. J. L. Morton, S. C. Benjamin, A. Ardavan, G. A. D. Briggs, J. W. Ager, and S. A. Lyon, *J. Phys.: Condens. Matter* **18**, S783 (2006).
- ³⁵N. Isailovic, M. Whitney, Y. Patel, J. Kubiatowicz, D. Copley, F. T. Chong, I. L. Chuang, and M. Oskin, *J. ACM* **1**, 34 (2004).
- ³⁶B. Koiller, X. Hu, and S. Das Sarma, *Phys. Rev. Lett.* **88**, 027903 (2001).
- ³⁷B. S. Song, S. Noda, T. Asano, and Y. Akahane, *Nature Mater.* **4**, 207 (2005).
- ³⁸N. Q. Vinh, P. T. Greenland, K. Litvinenko, B. Redlich, A. F. G.

- van der Meer, S. A. Lynch, M. Warner, A. M. Stoneham, G. Aeppli, D. J. Paul, C. R. Pidgeon, and B. N. Murdin, *Proc. Natl. Acad. Sci. U.S.A.* **105**, 10649 (2008).
- ³⁹W. Kohn, *Solid State Physics*, edited by F. Seits and D. Turnbull (Academic, New York, 1957), Vol. 5, p. 257.
- ⁴⁰A. K. Ramdas and S. Rodriguez, *Rep. Prog. Phys.* **44**, 1297 (1981).
- ⁴¹A. J. Mayur, M. D. Sciacca, A. K. Ramdas, and S. Rodriguez, *Phys. Rev. B* **48**, 10893 (1993).
- ⁴²A. Barenco, C. H. Bennett, R. Cleve, D. P. DiVincenzo, N. Margolus, P. Shor, T. Sleator, J. A. Smolin, and H. Weinfurter, *Phys. Rev. A* **52**, 3457 (2006).
- ⁴³K. Bergman, G. Grossmann, H. G. Grimmeiss, and M. Stavola, *Phys. Rev. Lett.* **56**, 2827 (1986).
- ⁴⁴H. G. Grimmeiss, E. Janzén, and K. Larsson, *Phys. Rev. B* **25**, 2627 (1982).
- ⁴⁵R. E. Peale, K. Muro, A. J. Sievers, and F. S. Ham, *Phys. Rev. B* **37**, 10829 (1988).
- ⁴⁶A. Debernardi, A. Baldereschi, and M. Fanciulli, *Phys. Rev. B* **74**, 035202 (2006).
- ⁴⁷D. Leibfried, R. Blatt, C. Monroe, and D. Wineland, *Rev. Mod. Phys.* **75**, 281 (2003).
- ⁴⁸D. Karaiskaj, J. A. H. Stotz, T. Meyer, M. L. W. Thewalt, and M. Cardona, *Phys. Rev. Lett.* **90**, 186402 (2003).
- ⁴⁹S. G. Pavlov, U. Bottger, H.-W. Hübers, R. K. Zhukavin, K. A. Kovalevsky, V. V. Tsyplenkov, V. N. Shastin, N. V. Abrosimov, and H. Riemann, *Appl. Phys. Lett.* **90**, 141109 (2007).
- ⁵⁰K. Hennessy, A. Badolato, M. Winger, D. Gerace, M. Atature, S. Gulde, S. Falt, E. L. Hu, and A. Imamoglu, *Nature (London)* **445**, 896 (2007).
- ⁵¹P. Clauws, J. Broeckx, E. Rotsaert, and J. Vennik, *Phys. Rev. B* **38**, 12377 (1988).
- ⁵²S. Das Sarma, R. de Sousa, X. Hu, and B. Koiller, *Solid State Commun.* **133**, 737 (2005).
- ⁵³S. G. Pavlov, R. Kh. Zhukavin, E. E. Orlova, V. N. Shastin, A. V. Kirsanov, H.-W. Hübers, K. Auen, and H. Riemann, *Phys. Rev. Lett.* **84**, 5220 (2000).
- ⁵⁴S. R. Schofield, N. J. Curson, M. Y. Simmons, F. J. Ruess, T. Hallam, L. Oberbeck, and R. G. Clark, *Phys. Rev. Lett.* **91**, 136104 (2003).
- ⁵⁵L. C. L. Hollenberg, A. D. Greentree, A. G. Fowler, and C. J. Wellard, *Phys. Rev. B* **74**, 045311 (2006).
- ⁵⁶A. Aspuru-Guzik, A. D. Dutoi, P. J. Love, and M. Head-Gordon, *Science* **309**, 1704 (2005).